

Role of magnetic resonance imaging in evaluating sphenoid sinus and internal carotid artery

H G HATIPOGLU, M A CETIN*, A SELVI, E YUKSEL

Abstract

Objective: This study aimed to determine whether magnetic resonance imaging has a role in the evaluation of the sphenoid sinus and internal carotid artery. In addition, we aimed to establish reference measurements for the minimal distance between the internal carotid arteries.

Method: The sphenoid sinuses and neighbouring internal carotid arteries of 90 patients were evaluated using sagittal T1-weighted and axial and coronal T2-weighted magnetic resonance images.

Results: Sphenoid sinus pneumatization was categorised as occipitosphenoïdal (0 per cent), conchal (3.3 per cent), presellar (14.4 per cent) or sellar (82.2 per cent). The internal carotid artery protruded into the sphenoid sinus in 32.8 per cent, with a septum in 9.4 per cent. The incidence of sellar-type sphenoid sinus pneumatization was higher in patients with protrusion of the internal carotid artery into the sphenoid sinus ($p < 0.001$). The incidence of presellar pneumatization was higher in patients without internal carotid artery protrusion ($p < 0.001$). The minimal distance between the internal carotid arteries varied between 9.04 and 24.26 mm (mean, 15.94 mm).

Conclusion: Magnetic resonance imaging can provide useful information about the sphenoid sinus and internal carotid artery, prior to endoscopic sphenoidotomy and trans-sphenoidal hypophysectomy.

Key words: Sphenoid Sinus; Magnetic Resonance-Imaging; Internal Carotid Artery; Anatomy

Introduction

The importance of pre-operative assessment of the sphenoid sinus and neighbouring neurovascular structures has risen following the introduction of new endoscopic techniques. One of the rare but major complications of the growing number of endoscopic sphenoidotomy and endoscopic endonasal trans-sphenoidal approach procedures used to remove pituitary tumours is severe haemorrhage due to parasphenoidal carotid artery trauma.¹ Therefore, it is essential pre-operatively to determine, as accurately as possible, the position of the internal carotid artery (ICA) in the lateral wall of the sphenoid sinus, in order to avoid intra-operative carotid injury.

It is challenging to evaluate the parasphenoidal structures with direct film X-rays and fluoroscopy. Currently, it has become routine to obtain a coronal computed tomography (CT) scan prior to endoscopic surgery. Anatomical variations of the sphenoid sinus and related anatomical structures have been demonstrated on gross anatomical and CT studies, with conflicting results.^{2–16} Magnetic resonance imaging (MRI) has advantages in pre-operative endoscopic planning, as it enables

delineation of the extent of soft tissue tumours.¹⁷ In dogs with a mass effect imaged by MRI, a diagnosis of neoplasia was significantly associated with vomer bone lysis, cribriform plate erosion, paranasal bone destruction, and sphenoid sinus and nasopharyngeal invasion by the mass; lack of a mass effect on MRI scans was significantly associated with inflammatory disease.¹⁸ Iatrogenic pseudoaneurysms of the ICA have been diagnosed on magnetic resonance angiography images.¹⁹ Intra-operative MRI during neurosurgical procedures (including trans-sphenoidal procedures for pituitary tumour removal) can assist the surgeon in safely removing the tumour.²⁰

Magnetic resonance imaging of the pituitary gland is undertaken pre-operatively for patients undergoing endoscopic trans-sphenoidal tumour removal. There is no radiation risk, and multiplanar imaging is possible. In this study, we sought to determine whether MRI scanning has a role in the evaluation of the sphenoid sinus and ICA. We also sought to establish reference measurements for the minimal distance between the internal carotid arteries, which we termed the 'internal carotid interval'. To pursue our research objectives, we reviewed a series of 90 consecutive cranial MRI studies.

From the Departments of Radiology and *Otorhinolaryngology, Head and Neck Surgery, Ankara Numune Education and Research Hospital, Turkey.

Accepted for publication: 18 May 2009. First published online 24 September 2009.

Materials and methods

A total of 167 patients undergoing cranial MRI were consecutively enrolled over a two-month period (June to July 2006). The scans were performed to investigate headache. Patients with a known pre-existing condition which might disturb the normal anatomy of the sphenoid and parasphenoidal structures, such as surgery or tumour with metastasis, were excluded from the study. Twenty-eight patients were thus excluded. In addition, 49 patients refused to participate in the study. Informed consent was obtained from all patients, following institutionally approved procedures, regulations and documentation. The study protocol was approved by our hospital's institutional review board. A total of 90 patients were included in the study, equating to a total of 180 sphenoid sinus sides.

The radiological anatomy of the sphenoid sinus and neighbouring structures was evaluated on cranial MRI studies. All examinations were performed on a 1.5 T, whole body MRI system (Excite; General Electric, Milwaukee, Wisconsin, USA) with a 33 mT/m maximum gradient capacity. The following images were obtained: spin echo, T1-weighted scans (TR, 500 msec; TE, 9.6 msec; slice thickness, 5 mm; interslice gap, 1.5 mm; FOV, 24 × 18 cm; matrix, 320 × 192; NEX, 2), and fast-recovery, fast spin echo, T2-weighted scans (TR, 4240 msec; TE, 98.1 msec; slice thickness, 5 mm; interslice gap, 1.5 mm; FOV, 24 × 18 cm; matrix, 352 × 224; NEX, 2).

Patients were classified according to their sphenoid sinus pneumatization type (assessed on midplane, sagittal, T1-weighted MRI scans) as follows: conchal, presellar, sellar and occipitosphe-noidal (Figure 1). The conchal type comprises a very small sinus which is separated from the sella turcica by a bony partition approximately 10 mm thick. The pre-sellar type consists of a sinus which does not extend posterior to a line running perpendicular to the sphenoidal plane through the tuberculum sellae. The sellar type consists of a sinus which extends behind the aforementioned line. Finally, the occipitosphe-noidal type comprises a sinus the pneumatization of which extends across the occipital synchondrosis.

Protrusion of the internal carotid artery (ICA) into the sphenoid sinus was noted. The degree of such protrusion was classified according to the percentage of artery diameter exposed, as 30–50 per cent, termed grade one, or 50–100 per cent, termed grade two. The sphenoidal septum or crest may extend and attach to the wall of the ICA protrusion; any such variation was noted (Figure 2a). The distance between both ICAs was calculated (Figure 2b and 2c). Pterygoid process pneumatization was deemed significant if it extended beyond a plane tangential to the most inferolateral aspect of the foramen rotundum and vidian canal in the axial and coronal planes. Anterior clinoid pneumatization in the axial and coronal planes was also noted.

All these evaluations were conducted on T2-weighted images; however, in seven cases the findings were confirmed on pre- or post-contrast T1-weighted images. Mucosal disease was evaluated

on T2-weighted images in all cases (Figure 3). All MRI images were assessed by three radiologists (HGH, AS, EY); any disagreements were discussed until consensus was achieved.

Statistical analysis

Data analysis was performed using the Statistical Package for the Social Sciences for Windows version 11.5 software. The Shapiro–Wilk test was used to determine whether the distributions of

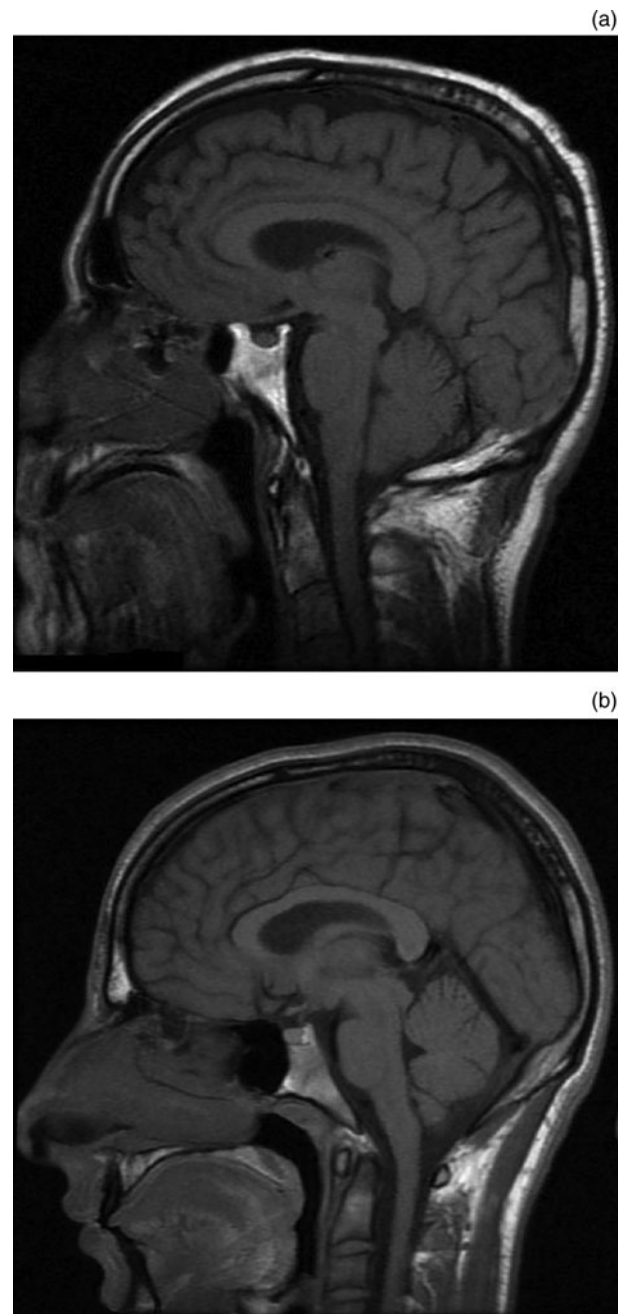


FIG. 1

Sagittal magnetic resonance imaging scan showing the types of sphenoid sinus pneumatization observed: (a) conchal; (b) presellar and (c) sellar. (A fourth type, occipitosphe-noidal, was also looked for but not observed.)

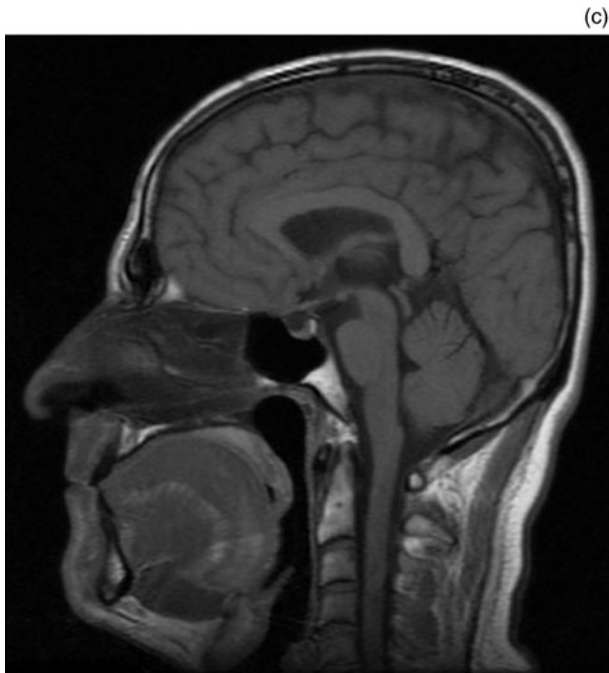


FIG. 1
Continued.

continuous variables were normal or not. Data were shown as mean \pm standard deviation (SD) for continuous variables. Categorical variables were presented as percentages. Means were compared using Student's *t*-test when the number of independent groups was two. Differences between the means of more than two groups were evaluated using one-way analysis of variance. Nominal data were analysed using the chi-square test or Fisher's exact test, where applicable. The McNemar test was applied for the comparison of the two sides. Odds ratios and 95 per cent confidence intervals (CIs) were calculated. A *p* value of less than 0.05 was considered statistically significant.

Results

The study included 90 patients (34 males and 56 females; mean age \pm SD, 42.92 \pm 18.94 years; age range 12–87 years). The following types of sphenoid sinus pneumatization were observed: conchal type in three patients (3.3 per cent); presellar type in 13 (14.4 per cent); sellar type in 74 (82.2 per cent); and occipitosphenoïdal type in none (0 per cent).

Data on the incidence and degree of internal carotid artery (ICA) protrusion are summarised in Table I.

We observed sphenoidal septum or crest attachment to a right-sided ICA protrusion in eight patients (8.9 per cent) and to a left-sided ICA protrusion in nine patients (10 per cent); such attachment occurred in 17 patients (18.9 per cent) in total. There was no statistically significant difference in the occurrence of sphenoidal septum or crest attachment to an ICA protrusion, comparing the right and left sides (*p* = 1.000).

The closest distance between the right and left internal carotid arteries in the parasphenoidal region varied between 9.04 and 24.26 mm. The mean \pm SD for this parameter was 16.18 \pm 3.20 mm for female patients (range, 9.40–23.82 mm) and 15.56 \pm 3.70 mm for male patients (range, 9.04–24.26 mm). There were no statistically significant differences between the means of this parameter, comparing the two genders (*p* = 0.401).

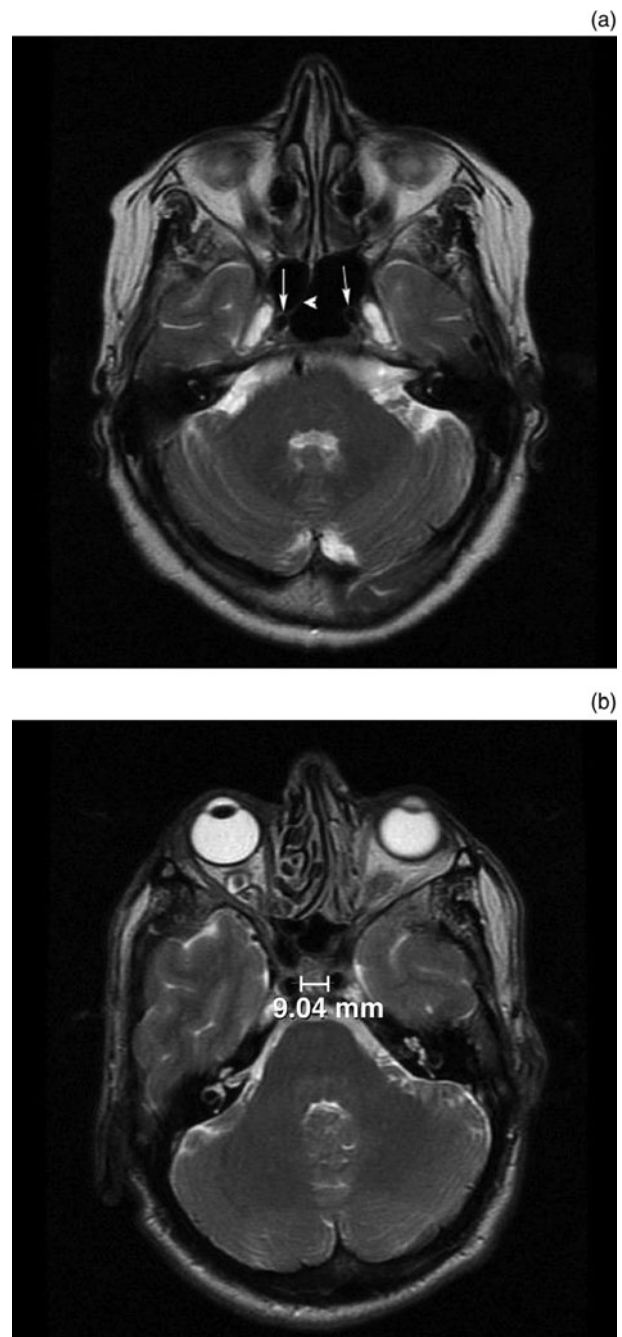


FIG. 2

Axial magnetic resonance imaging scans showing (a) protrusion of the internal carotid arteries into the sphenoid sinus (arrows); a septum or crest (arrowhead) is attached on the right side. Also shown are the (b) shortest and (c) longest internal carotid intervals detected.

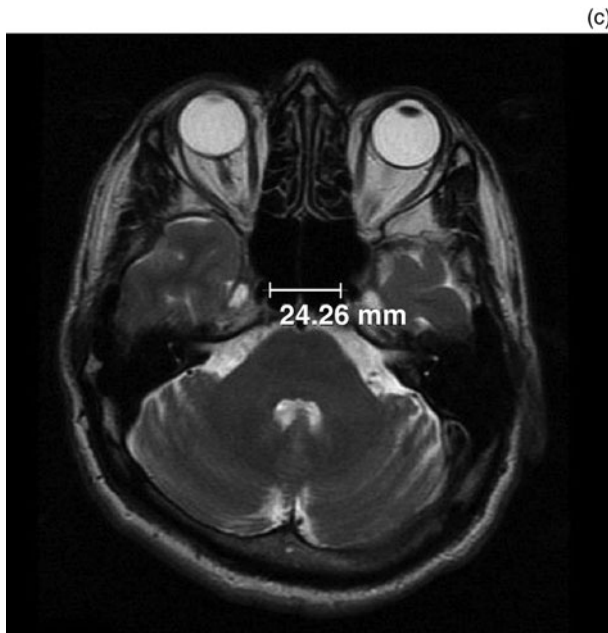


FIG. 2
Continued.

Anterior clinoid pneumatisation was observed in 16 patients (17.8 per cent) and pterygoid process pneumatisation in 32 patients (35.5 per cent) (Table II). The presence of anterior clinoid pneumatisation was found to be a predictive factor associated with ICA protrusion only on the right side (odds ratio, 5.62; 95 per cent CI, 1.57–20.18; $p = 0.009$). The presence of pterygoid process pneumatisation was found to be a predictive factor associated with

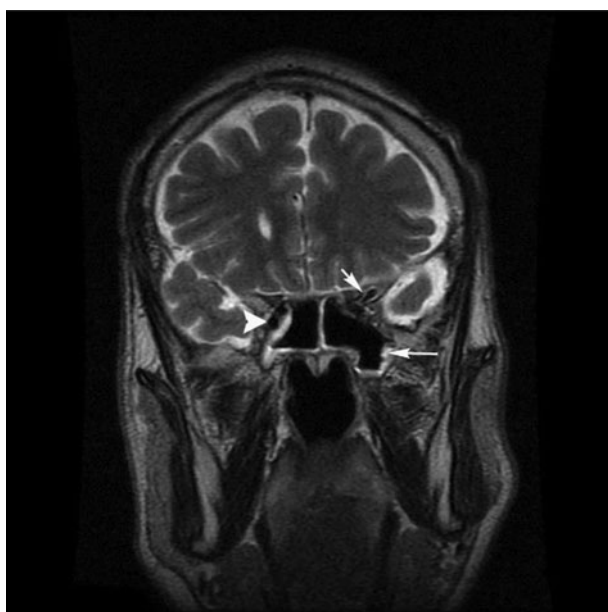


FIG. 3

Coronal, T2-weighted magnetic resonance imaging scan showing pneumatisation of the left anterior clinoid process (short arrow) and left pterygoid plate (long arrow). There is also protrusion of the right internal carotid artery (arrowhead). Note the mucosal disease on both sides.

(c)

TABLE I

INCIDENCE OF INTERNAL CAROTID ARTERY PROTRUSION INTO SPHENOID SINUS

R protrusion grade	L protrusion grade (<i>n</i> (%))			Total
	0	1	2	
0	53 (58.9)	4 (4.4)	2 (2.2)	59 (65.6)
1	5 (5.6)	3 (3.3)	2 (2.2)	10 (11.1)
2	4 (4.4)	2 (2.2)	15 (16.7)	21 (23.3)
Total	62 (68.9)	9 (10.0)	19 (21.1)	90 (100)

Data represent patients. R = right side; L = left side

TABLE II

INCIDENCE OF SPHENOID SINUS PNEUMATISATION

Right side	Left side (<i>n</i> (%))		
	-	+	Total
<i>Anterior clinoid</i>			
-	74 (82.2)	3 (3.3)	77 (85.6)
+	6 (6.7)	7 (7.8)	13 (14.4)
Total	80 (88.9)	10 (11.1)	90 (100)
<i>Pterygoid process</i>			
-	58 (64.4)	8 (8.9)	66 (73.3)
+	4 (4.4)	20 (22.2)	24 (26.7)
Total	62 (68.9)	28 (31.1)	90 (100)

Data represent patients. - = pneumatisation absent; + = pneumatisation present

both right-sided and left-sided ICA protrusion (for right side: odds ratio 6.80, 95 per cent CI 2.44–18.96, $p < 0.001$; for left side, odds ratio 4.35, 95 per cent CI 1.66–11.38, $p = 0.002$).

There was no statistically significant difference in the mean internal carotid interval, comparing patients with and without ICA protrusion ($p = 0.548$). Table III summarises these findings.

There was no statistically significant association between anterior clinoid pneumatisation and age ($p = 0.758$). However, patients with pterygoid process pneumatisation were found to be younger on average than those without ($p = 0.009$). There was no statistically significant association between pterygoid process pneumatisation and patient sex ($p = 0.646$). However, anterior clinoid pneumatisation was more frequent in males ($p = 0.004$). The presence of mucosal disease had no statistically significant association with either pterygoid process pneumatisation ($p = 0.274$) or anterior clinoid pneumatisation ($p = 0.470$). Please refer to Table IV for detailed analysis.

There was no statistically significant association between sphenoid sinus pneumatisation and either patients' sex ($p = 0.986$) or age ($p = 0.650$). There was also no statistically significant association between the internal carotid interval and the presence of sphenoid sinus pneumatisation ($p = 0.538$) (Table V).

The incidence of sellar-type sphenoid sinus pneumatisation was higher in patients with ICA protrusion, compared with those without ($p < 0.001$). Presellar-type sphenoid sinus pneumatisation was found in patients without ICA protrusion, but did

TABLE III

INTERNAL CAROTID ARTERY PROTRUSION INTO SPHENOID SINUS, BY ANTERIOR CLINOID AND PTERYGOID PROCESS PNEUMATISATION AND INTERNAL CAROTID INTERVAL

Variable	ICA protrusion (<i>n</i> (%))		<i>p</i>	OR (95% CI)
	–*	+†		
<i>Right side</i>				
ACP –	55 (93.2)	22 (71.0)	0.009	1‡
ACP +	4 (6.8)	9 (29.0)		5.62 (1.57–20.18)
PPP –	51 (86.4)	15 (48.4)	<0.001	1‡
PPP +	8 (13.6)	16 (51.6)		6.80 (2.44–18.96)
ICI (mean ± SD; mm)	16.0 ± 3.3	15.8 ± 3.6	0.811	0.98 (0.86–1.12)
<i>Left side</i>				
ACP –	56 (90.3)	24 (85.7)	0.495	1‡
ACP +	6 (9.7)	4 (14.3)		1.56 (0.40–6.01)
PPP –	49 (79.0)	13 (46.4)	0.002	1‡
PPP +	13 (21.0)	15 (53.6)		4.35 (1.66–11.38)
ICI (mean ± SD; mm)	16.1 ± 3.5	15.5 ± 3.2	0.403	0.94 (0.82–1.08)

Data represent patients unless otherwise specified. *Right side, *n* = 59; left side, *n* = 62. †Right side, *n* = 31; left side, *n* = 28. ‡Reference category. ICA = internal carotid artery; OR = odds ratio; CI = confidence intervals; ACP = anterior clinoid pneumatization; PPP = pterygoid plate pneumatization; – = absent; + = present; ICI = closest distance between right and left ICAs in parasphenoidal region; SD = standard deviation

TABLE IV

ANTERIOR CLINOID AND PTERYGOID PLATE PNEUMATISATION BY PATIENT AGE, SEX AND PRESENCE OF MUCOSAL DISEASE

Variable	Right side		<i>p</i>	Left side		<i>p</i>
	Pneumatization			Pneumatization		
	–	+		–	+	
<i>ACP</i>						
Age (mean ± SD; yr)	43.1 ± 19.2	42.1 ± 18.0	0.863	43.1 ± 18.4	41.4 ± 24.1	0.789
Female sex (<i>n</i> (%))	51 (66.2)	5 (38.5)	0.069	53 (66.3)	3 (30.0)	0.038
MD (<i>n</i> (%))	16 (20.8)	2 (15.4)	1.000	18 (22.5)	1 (10.0)	0.682
<i>PPP</i>						
Age (mean ± SD; yr)	45.0 ± 18.8	37.2 ± 18.6	0.084	45.5 ± 18.1	37.1 ± 19.8	0.050
Female sex (<i>n</i> (%))	42 (63.6)	14 (58.3)	0.646	39 (62.9)	17 (60.7)	0.843
MD (<i>n</i> (%))	14 (21.2)	4 (16.7)	0.771	15 (24.2)	4 (14.3)	0.286

– = absent; + = present; ACP = anterior clinoid pneumatization; PPP = pterygoid plate pneumatization; SD = standard deviation; yr = years; MD = mucosal disease

TABLE V

SPHENOID SINUS PNEUMATISATION PATTERN BY PATIENT AGE, SEX AND INTERNAL CAROTID INTERVAL

Variable	Conchal*	Sellar†	Presellar‡	<i>p</i>
Age (mean ± SD; yr)	43.0 ± 13.8	42.1 ± 19.2	47.5 ± 19.0	0.650
Female sex (<i>n</i> (%))	2 (66.7)	46 (62.2)	8 (61.5)	0.986
ICI (mean ± SD; mm)	15.3 ± 4.6	15.8 ± 3.3	16.9 ± 3.6	0.538

**n* = 3; †*n* = 74; ‡*n* = 13. SD = standard deviation; yr = years; ICI = closest distance between right and left internal carotid arteries in parasphenoidal region

not occur in those with ICA protrusion (*p* < 0.001) (Table VI).

Discussion

The sphenoid sinus continues to pneumatise until adolescence.²¹ In adulthood, the extent of sphenoidal pneumatization is classified as conchal, presellar, sellar or occipitosphenoidal (Table VII).^{3,4} The current study assessed sphenoidal pneumatization patterns on sagittal, T1-weighted MRI scans. In our

patients, the extent of pneumatization was not related to age or sex. Sellar pneumatization was the most frequent type. As the degree of sphenoid sinus pneumatization increases, the surrounding neurovascular structures project more into the sinus cavity, appearing as ridges. This may increase the risk of vessel and nerve injury during sphenoidotomy procedures.

Using sagittal, T1-weighted MRI scanning, it is possible to evaluate the thickness of the posterior wall of the sphenoid sinus. In patients with a pituitary

TABLE VI

INTERNAL CAROTID ARTERY PROTRUSION INTO SPHENOID SINUS, BY SPHENOID SINUS PNEUMATISATION PATTERN

Pattern	ICA protrusion (n (%))	
	–*	+†
<i>R side</i>		
Conchal	3 (5.1)	0 (0)
Sellar	43 (72.9)	31 (100.0)
Presellar	13 (22.0)	0 (0)
<i>L side</i>		
Conchal	3 (4.8)	0 (0)
Sellar	46 (74.2)	28 (100.0)
Presellar	13 (21.0)	0 (0)

*Right side, n = 59; left side, n = 62. †Right side, n = 31; left side, n = 28. ICA = internal carotid artery; R = right; L = left

mass who may require a trans-sphenoidal surgical approach, the posterior extent of the main sphenoid sinus cavity should be carefully evaluated. If more than 1 or 2 mm of bone remains between the posterior margin of the pneumatized sinus and the anterior sellar wall (this occurs in less than 1 per cent of cases), surgeons should consider avoiding a transnasal, trans-sphenoidal hypophysectomy. A thick, bony posterior sinus wall may also be a relative contraindication.²² However, with the current, widespread use of high speed drilling, these operations can be performed much more safely.

The lateral wall of the sphenoid sinus is related to the orbital apex, optic canal, optic nerve, cavernous sinus and internal carotid artery.²² Surgeons should consider these important neighbouring neurovascular structures and take into consideration the possible anatomical variations, prior to any dissection in this region. Injuries of the internal carotid artery (ICA) may occur, not only due to anomalies and aneurysms of the artery, but also in cases of a missing bony covering of the artery in the sphenoid sinus when the sinus is not opened strictly parasagittally.⁹ In the latter case, tamponade compression or balloon occlusion of the ICA may be the only options. However, hemiplegia or death is the result in most such cases.¹ On CT scans, the ICA, the optic nerve, and the more posterior cavernous sinus and its contents are only visualisable as indentations on the lateral walls of the sphenoid bone, depending on the degree of sphenoid sinus pneumatization. However, on MRI, the ICA can be distinguished from the cavernous sinus surrounding it. Vascular anomalies and aneurysms can be diagnosed on MRI and MR angiography images.¹⁹

The current study attempted to establish reference measurements for the minimal distance between the internal carotid arteries, termed the internal carotid interval. The closest distance between the internal carotid arteries in the parasphenoidal region varied between 9.04 and 24.26 mm. There was no statistically significant difference in this parameter between male and female patients. Furthermore, there was no statistically significant difference in the internal carotid interval between patients with and without ICA protrusion.

Various studies have reported ICA protrusion into the sphenoid sinus in between 5.2 and 72 per cent of cases.^{8,9,11,13–16} In our study, almost one-third (32.8 per cent) of our patients had ICA protrusion into the sphenoid sinus. The prevalence of sellar-type sphenoid pneumatization was significantly greater in patients with ICA protrusion, and the prevalence of presellar-type pneumatization was significantly greater in patients without ICA protrusion. Because of the high incidence of ICA protrusion into the sphenoid sinus, surgeons and radiologists should be aware of the degree of such protrusion prior to sphenoidotomy.

- **Pre-operative assessment of the sphenoid sinus and neighbouring neurovascular structures has gained importance following the introduction of new endoscopic techniques**
- **Magnetic resonance imaging provides reliable information on anatomical variations of the sphenoid sinus**
- **This information could help avoid intra-operative carotid injury during endoscopic sphenoid sinus and trans-sphenoidal pituitary gland procedures**

In our study, bony septum attachment to a protruding ICA was better evaluated on axial MRI scans. We observed this anatomical variant in 18.9 per cent of our patients; other authors have reported an incidence of 5.4 to 26.7 per cent.^{8,14–16} This variant is usually present at the site of fusion of several synchondroses of the sphenoid bone.⁸ It may result in carotid avulsion during surgery.¹

We found anterior clinoid pneumatization and pterygoid process pneumatization in 17.8 and 35.5 per cent of patients, respectively. Other authors have reported incidences of 6 to 24.1 per cent for

TABLE VII

PREVIOUSLY REPORTED INCIDENCES OF SPHENOID SINUS PNEUMATISATION TYPES

Study	Sellar (%)	Presellar (%)	Conchal (%)	Occipitospheoidal (%)
Banna & Olutola ⁶	85.7	11.4	2.85	0
Johnson <i>et al.</i> ⁹	64.2	32.4	3.2	–
Hammer & Radberg ³	86	11	2.5	–
Kinnman ⁵	88	11.2	–	–
Hatipoglu <i>et al.</i> [*]	79.27	18.91	1.8	0

*Current study. – = not assessed

anterior clinoid pneumatization and of 29.3 to 39.7 per cent for pterygoid process pneumatization.^{13–16} We found the presence of pterygoid process pneumatization to be a predictive factor associated with ICA protrusion. In contrast, other authors have found no statistically significant association between pterygoid process pneumatization and ICA protrusion.^{14–16}

The literature gives conflicting accounts of the anatomy of the sphenoid sinus. Such variation may be the result of the number of patients studied, racial or population variability, or differences in methodology. On plain X-ray films, the sphenoid sinus cavity is best evaluated on the lateral, base and open-mouth Waters views. However, overlapping of structures may make assessment difficult. On CT views, neurovascular structures can be evaluated only as indentations of the cavernous sinus. On MRI views, however, it is possible to distinguish the carotid artery from the cavernous sinus surrounding it. The internal carotid arteries may be visualised along their whole length. The current study assessed patients who underwent MRI as an investigation for headaches. Therefore, paranasal sinus findings were incidental. Previously reported CT studies of sphenoid sinus anatomy used patients complaining of sinusitis; this may have created a bias. However, the current study also had several limitations. Computed tomography evaluates sinus disease and bony dehiscence more reliably.

Conclusion

Magnetic resonance imaging provides reliable information on variations of sphenoid sinus anatomy. In addition, MRI makes it possible to distinguish the internal carotid artery (ICA) from the cavernous sinus surrounding it. This information could help surgeons to avoid intra-operative ICA injury during endoscopic sphenoid sinus and trans-sphenoidal pituitary gland procedures. The distance between the ICAs, which we termed the internal carotid interval, can be as small as 9 mm in both genders. The internal carotid interval is not influenced by patients' sex or age, or by the pneumatization pattern of the sphenoid sinus. There is no statistically significant association between the internal carotid interval and the degree of ICA protrusion into the sphenoid sinus. The sphenoid pneumatization pattern, and the posterior sphenoid sinus wall, may be assessed quite accurately on sagittal, T1-weighted MRI scans. The incidence of sellar-type pneumatization is greater in patients with ICA protrusion.

References

- Hudgins PA. Complications of endoscopic sinus surgery. The role of the radiologist in prevention. *Radiol Clin North Am* 1993;**31**:21–32
- Van Alyea OE. Sphenoid sinus. Anatomic study, with consideration of the clinical significance of the structural characteristics of the sphenoid sinus. *Arch Otolaryngol* 1941;**34**:225–53
- Hammer G, Radberg C. The sphenoid sinus. An anatomic and roentgenologic study with reference to transsphenoidal hypophysectomy. *Acta Radiol* 1961;**56**:401–22

- Hamberger CA, Hammer G, Norlen G, Sjogren B. Trans-antrosphenoidal hypophysectomy. *Arch Otolaryngol* 1961;**74**:2–8
- Kinnman J. Surgical aspects of the anatomy of the sphenoidal sinuses and the sella turcica. *J Anat* 1977;**124**:541–53
- Banna M, Olutola PS. Patterns of pneumatization and septation of the sphenoidal sinus. *J Can Assoc Radiol* 1983;**34**:291–3
- Fujii K, Chambers SM, Rhoton AL Jr. Neurovascular relationships of the sphenoid sinus. A microsurgical study. *J Neurosurg* 1979;**50**:31–9
- Elwany S, Elsaedi I, Thabet H. Endoscopic anatomy of the sphenoid sinus. *J Laryngol Otol* 1999;**113**:122–6
- Johnson DM, Hopkins RJ, Hanafiee WN, Fisk JD. The unprotected parasphenoidal carotid artery studied by high-resolution computed tomography. *Radiology* 1985;**155**:137–41
- Kron TK, Johnson CM 3rd. Diagnosis and management of the opacified sphenoid sinus. *Laryngoscope* 1983;**93**:1319–27
- Teatini G, Simonetti G, Salvolini U, Masala W, Meloni F, Rovasio S *et al.* Computed tomography of the ethmoid labyrinth and adjacent structures. *Ann Otol Rhinol Laryngol* 1987;**96**:239–50
- Basak S, Karaman CZ, Akdilli A, Mutlu C, Odabasi O, Erpek G. Evaluation of some important anatomical variations and dangerous areas of the paranasal sinuses by CT for safer endonasal surgery. *Rhinology* 1998;**36**:162–7
- Arslan H, Aydinlioglu A, Bozkurt M, Egeli E. Anatomic variations of the paranasal sinuses: CT examination for endoscopic sinus surgery. *Auris Nasus Larynx* 1999;**26**:39–48
- Sirikci A, Bayazit YA, Bayram M, Mumbuc S, Gungor K, Kanlikama M. Variations of sphenoid and related structures. *Eur Radiol* 2000;**10**:844–8
- Kazkayasi M, Karadeniz Y, Arikan OK. Anatomic variations of the sphenoid sinus on computed tomography. *Rhinology* 2005;**43**:109–14
- Unal B, Bademci G, Bilgili YK, Batay F, Avci E. Risky anatomic variations of sphenoid sinus for surgery. *Surg Radiol Anat* 2006;**28**:195–201
- Som PM, Costantino PD, Silvers AR. Imaging central skull base neural tumor spread from paranasal sinus malignancies: a critical factor in treatment planning. *Skull Base Surg* 1999;**9**:15–21
- Miles MS, Dhaliwal RS, Moore MP, Reed AL. Association of magnetic resonance imaging findings and histologic diagnosis in dogs with nasal disease: 78 cases (2001–2004). *J Am Vet Med Assoc* 2008;**232**:1844–9
- Buerke B, Tombach B, Stoll W, Heindel W, Niederstadt T. Magnetic resonance angiography follow-up examinations to detect iatrogenic pseudoaneurysms following otorhinolaryngological surgery. *J Laryngol Otol* 2007;**121**:698–701
- Anand VK, Schwartz TH, Hiltzik DH, Kacker A. Endoscopic transsphenoidal pituitary surgery with real-time intraoperative magnetic resonance imaging. *Am J Rhinol* 2006;**20**:401–5
- Warwick R, Williams PL. *Gray's Anatomy*, 35th edn. London: Longmans, 1973
- Som P, Shugar JMA, Brandwein SM. Anatomy and physiology. In: Som PM, Curtin HD, eds. *Head and Neck Imaging*, 4th edn. St Louis: Mosby, 2003;87–147

Address for correspondence:
Dr Hatice Gul Hatipoglu,
Maresal Fevzi Cakmak cad 64/A,
Besevler 06500,
Ankara, Turkey.

Fax: 03122128410
E-mail: gulhatip@yahoo.com

Dr H G Hatipoglu takes responsibility for the integrity of the content of the paper.
Competing interests: None declared
